Magnetoencephalography-detected Phase-amplitude Coupling in Parkinson Disease

Masataka Tanaka
Department of Neurosurgery, Osaka University Graduate School of Medicine
Takufumi Yanagisawa (tyanagisawa@nsurg.med.osaka-u.ac.jp)
Institute for Advanced Co-Creation Studies, Osaka University
Ryohei Fukuma
Department of Neurosurgery, Osaka University Graduate School of Medicine
Naoki Tani
Department of Neurosurgery, Osaka University Graduate School of Medicine
Satoru Oshino
Department of Neurosurgery, Osaka University Graduate School of Medicine
Masahito Mihara
Department of Neurology, Osaka University Graduate School of Medicine
Noriaki Hattori
Department of Neurology, Osaka University Graduate School of Medicine
Yuta Kajiyama
Department of Neurology, Osaka University Graduate School of Medicine
Ryota Hashimoto
Department of Pathology of Mental Diseases, National Institute of Mental Health, National Center of Neurology and Psychiatry
Manabu Ikeda
Department of Psychiatry, Osaka University Graduate School of Medicine
Hideki Mochizuki
Department of Neurology, Osaka University Graduate School of Medicine
Haruhiko Kishima
Department of Neurosurgery, Osaka University Graduate School of Medicine

Research Article

Keywords: Parkinson disease, cortico-basal circuit , hypothesized , magnetoencephalography

Posted Date: July 22nd, 2021

DOI: https://doi.org/10.21203/rs.3.rs-732684/v1

Title:

Magnetoencephalography-detected phase-amplitude coupling in Parkinson disease

Short Running Title:

Resting-State PAC in PD

Authors:

Masataka Tanaka,[1] Takufumi Yanagisawa,[1–3]* Ryohei Fukuma,[1,3] Naoki Tani,[1] Satoru Oshino,[1] Masahito Mihara,[4] Noriaki Hattori,[4] Yuta Kajiyama,[4] Ryota Hashimoto,[5–7] Manabu Ikeda,[6] Hideki Mochizuki,[4] Haruhiko Kishima[1]

Affiliations:

[1]Department of Neurosurgery, Osaka University Graduate School of Medicine, 2-2 Yamadaoka, Suita, Osaka 565-0871 Japan

[2]Institute for Advanced Co-Creation Studies, Osaka University, 2-2 Yamadaoka, Suita, Osaka 565-0871 Japan

[3]ATR Computational Neuroscience Laboratories, Department of Neuroinformatics, 2-2-2 Hikaridai, Seika-cho, Kyoto 619 0288 Japan

[4]Department of Neurology, Osaka University Graduate School of Medicine, 2-2 Yamadaoka, Suita, Osaka 565-0871 Japan

[5]Department of Pathology of Mental Diseases, National Institute of Mental Health, National Center of Neurology and Psychiatry, 4-1 Ogawahigashi, Kodaira, Tokyo 187-8553 Japan

[6]Department of Psychiatry, Osaka University Graduate School of Medicine, 2-2 Yamadaoka, Suita, Osaka 565-0871 Japan

[7]Molecular Research Center for Children's Mental Development, United Graduate School of Child Development, Osaka University, 2-2 Yamadaoka, Suita, Osaka 565-0871 Japan

Abstract

To characterize Parkinson disease, abnormal phase-amplitude coupling is assessed in the cortico-basal circuit using invasive recordings. Whether the same phenomenon might be found in areas other than the cortico-basal ganglia circuit is unknown. We hypothesized that using magnetoencephalography to assess phase-amplitude coupling in the whole brain can characterize Parkinson disease. We recorded resting-state magnetoencephalographic signals in patients with Parkinson disease and in healthy age- and sex-matched participants. We compared the whole-brain signals from the two groups, evaluating the power spectra of 3 frequency bands (alpha, 8–12 Hz; beta, 13–25 Hz; gamma, 50–100 Hz) and the coupling between the gamma amplitude and the alpha or beta phases. Compared with the healthy participants, the patients with Parkinson disease showed significant beta–gamma phase-amplitude coupling in the sensorimotor, occipital, and temporal cortices. In contrast, the two groups showed no significant difference in their resting-state powers. Further, in a resting state, the beta–gamma phase-amplitude coupling in the sensorimotor cortices correlated significantly with motor symptoms of Parkinson disease ($P < 0.05$); the beta-band power did not. We thus demonstrated that beta–gamma phase-amplitude coupling in the resting state characterizes Parkinson disease.

Introduction

Dysrhythmia contributes to the motor symptoms of Parkinson disease. In previous studies, patients with Parkinson disease in a resting state were observed to have abnormal

synchronization in cortico-basal ganglia circuits, including the subthalamic nucleus, globus pallidus internus, and primary motor cortex[1,2]. Beta oscillations in the subthalamic nucleus have been correlated with motor symptoms such as bradykinesia and rigidity[3,4], although recent evidence has been contradictory[5]. Excessive beta oscillations in the cortico-basal ganglia circuit have been shown to represent pathologic oscillations in Parkinson disease.

The beta oscillation phase measured during a resting state in patients with Parkinson disease has been significantly coupled with the gamma oscillation (>50 Hz) amplitude in the subthalamic nucleus[6,7] and motor cortex[8,9], termed beta–gamma phase-amplitude coupling (PAC)[10,11]. Cortical beta–gamma PAC has been correlated with Parkinsonian motor symptoms and is attenuated by deep brain stimulation and levodopa[12]. During movement, PAC attenuated earlier in patients with Parkinson disease than in study participants without movement disorders[9]. Excessive beta oscillations and beta–gamma PAC in the cortico-basal ganglia circuit are therefore potential cortical biomarkers of Parkinsonian motor symptoms[13].

Previous evaluations of PAC mostly used intracranial electrodes in the cortico-basal ganglia circuit, such as electrodes for deep brain stimulation or subdural electrodes on the sensorimotor cortex to measure electrocorticographic signals. Whether the PAC in the gamma oscillation in patients with Parkinson disease differs from that in healthy study participants (HSPs) of similar ages has not been well examined. Although some studies using electroencephalography revealed exaggerated PAC in Parkinson disease, anatomic differences in PAC have not been compared because of the low spatial resolution of electroencephalography[14,15]. However, recent studies showed that magnetoencephalography (MEG) can evaluate cortical PAC with high reliability[16–18]. We therefore recorded MEG signals to evaluate PAC during a resting state both in patients

with Parkinson disease and in age-matched HSPs. We hypothesized that beta–gamma PAC estimated from MEG signals characterizes patients with Parkinson disease and thus acts as a biomarker for Parkinsonian motor symptoms.

Results

Participants Between May 2015 and February 2018, 32 patients with Parkinson disease and 54 HSPs were recruited at Osaka University Hospital in Japan. Before data analysis, 9 patients and 17 HSPs were excluded: 2 patients and 5 HSPs because they fell asleep or moved during the resting-state recording; 2 patients and 7 HSPs because of metal artefact contamination; 1 patient and 5 HSPs because of equipment trouble; and 4 patients because of another movement disorder (essential tremor) or motor impairment (limb paresis caused by polio) and a change in diagnosis to multiple system atrophy. The subsequent analyses included the remaining 23 patients with Parkinson disease (11 men; mean age: 65.3 ± 7.9 years; Table 1) and 23 of the remaining 37 HSPs, age- and sex-matched to the patients (11 men; mean age: 62.8 ± 5.7 years).

Table 1. Clinical characteristics of the participants with Parkinson disease

Patients		Age (years)	More affected side	MDS-UPDRS-III akinesia score	On/off state during recording	LEDD (mg/dL)	Disease duration (years)
ID	Sex						
1	Female	68	Right	8	On	625	5
2	Female	76	Right	5	On	0	1
3	Male	73	Left	13	On	0	4
4	Male	54	Left	5	On	340	3
5	Female	72	Left	4	On	37.5	30
6	Female	69	Left	7	On	175	4
7	Male	75	Left	17	On	400	8
8	Male	69	Left	12	Off	1,406	15
9	Female	70	Left	9	On	891.5	10
10	Female	52	Left	1	On	715	11
11	Female	72	Left	15	On	100	1
12	Male	69	Left	12	On	110	4
13	Male	54	Right	14	Off	1,344.5	11
14	Female	68	Right	7	On	100	4
15	Male	63	Left	19	On	1,037.5	7
16	Female	55	Right	20	Off	560	6
17	Male	64	Left	12	On	0	3
18	Female	69	Left	8	On	200	5
19	Female	72	Left	14	On	975	18
20	Male	52	Left	13	On	549	4
21	Male	53	Right	11	On	1,081	18
22	Male	66	Left	14	On	752.2	8
23	Female	66	Left	21	Off	948	5

MDS-UPDRS-III akinesia score = sum of akinesia-related scores on the Movement Disorder Society–sponsored revision of the Unified Parkinson's Disease Rating Scale, part III; LEDD = levodopa equivalent daily dose.

Beta–gamma PAC characterizes Parkinson disease To estimate PAC during the resting state, we evaluated a synchronization index (SI)[19] for gamma-band amplitude and alpha- or beta-band phases at each cortical area. Patients with Parkinson disease had SI values for beta–gamma PAC in the sensorimotor, occipital, and temporal cortices that

were significantly higher than the shuffled SI values (Figure 1A; $P < 0.05$, 2-tailed Welch *t*-test, false discovery rate corrected). In contrast, the HSPs had significant beta–gamma PACs in a part of the motor cortices (Figure 1B). The exaggerated beta–gamma PAC during the resting state was noninvasively observed in the patients with Parkinson disease. The supplementary material details the areas in which significant beta–gamma PAC was observed. No significant alpha–gamma PAC during the resting state was observed in either the patients with Parkinson disease or the HSPs.

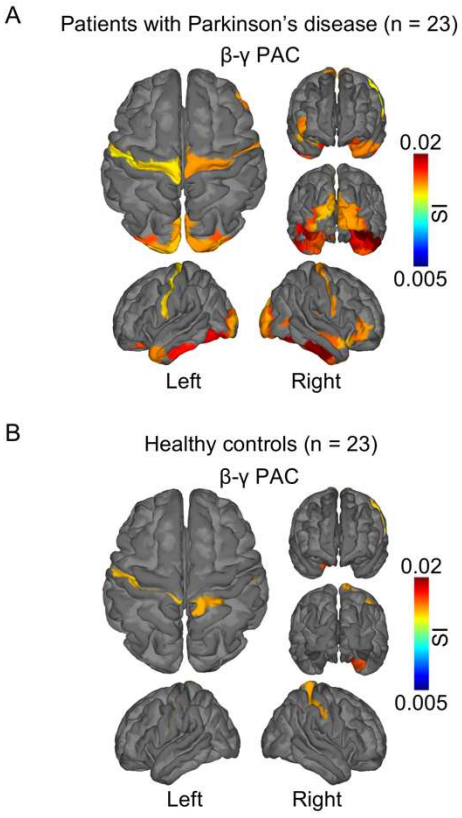

Figure 1. Beta–gamma phase-amplitude coupling during the resting state. For each study group (patients with Parkinson disease and healthy matched participants), we averaged the gamma amplitude and beta phase synchronization index values and color-coded the cortex of (A) patients (n = 23) and (B) healthy participants (n = 23). Synchronization index values are shown only if they exceeded the shuffled values.

The cortical power of 3 frequency bands (alpha, beta, and gamma) was also evaluated at each cortical area (Figure 2). In each frequency band, the power of the individual cortical areas did not significantly differ between the groups (patients compared with HSPs: $P > 0.05$; 3 frequency bands: $P > 0.05$; interaction: $P > 0.05$; 2-way analysis of variance, false discovery rate corrected).

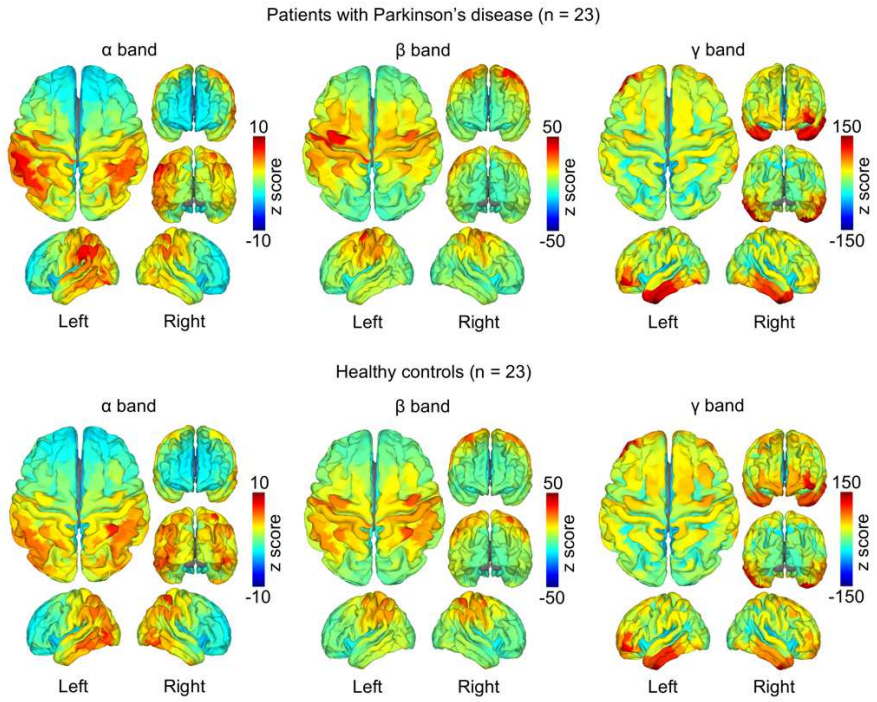

Figure 2. Cortical power during the resting state. We averaged the normalized power of 3 frequency bands (alpha, beta, and gamma) for each study group (patients with Parkinson disease and healthy matched participants), and we color-coded each cortical area in the patients (n = 23) and the healthy participants (n = 23).

Beta–gamma PAC correlates with motor symptoms of Parkinson disease We evaluated the correlation between beta–gamma PAC in the sensorimotor cortices and akinesia as scored using part III of the Movement Disorder Society–sponsored revision of the Unified Parkinson's Disease Rating Scale (MDS-UPDRS-III) for the patients with Parkinson disease (Figure 3). The averaged SI values of beta–gamma PAC in the early somatosensory and motor cortices in which significant beta–gamma PAC was present correlated with the MDS-UPDRS-III scores for akinesia (Pearson correlation coefficient: $r = 0.45$, $P = 0.022$; Figure 3A). However, the averaged Z scores of the beta-band power in the same area did not correlate with the MDS-UPDRS-III scores for akinesia ($r = -0.02$, $P = 0.943$; Figure 3B).

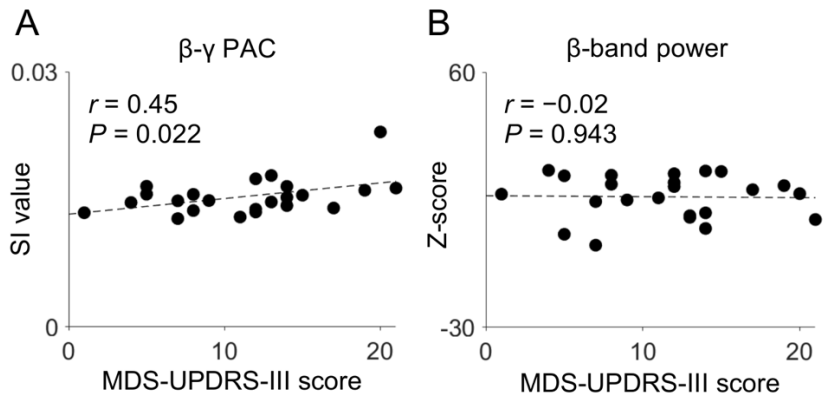

Figure 3. Correlations between disease symptoms and beta–gamma phase-amplitude coupling or beta-band power . (A) Correlation between averaged synchronization index values for the sensorimotor areas in which significant phase-amplitude coupling is present and the sum of the MDS-UPDRS-III scores for akinesia. (B) Correlation between the averaged Z scores for the sensorimotor areas and the sum of the MDS-UPDRS-III scores for akinesia. In the plots, each dot represents a patient with Parkinson disease (n = 23); a dashed least-squares lineis also shown. MDS-UPDRS-III = Movement Disorder Society–sponsored revision of the Unified Parkinson Disease Rating Scale, part III.

Discussion

By evaluating MEG signals in the resting state, we demonstrated that beta–gamma PAC in the sensorimotor, occipital, and temporal cortices characterizes patients with Parkinson disease. Moreover, the motor symptoms of Parkinson disease as evaluated by MDS-UPDRS-III scores are significantly correlted with resting-state beta–gamma PAC in the sensorimotor cortex, independent of beta-band power. Those results are consistent with findings in previous studies that used invasive measurement techniques, suggesting that, during the resting state, beta–gamma PAC in the precentral gyrus is exaggerated in patients with Parkinson disease[8]. Using non-invasive MEG signals, we demonstrated that beta–gamma PAC during the resting state is a biomarker predicting motor symptoms in Parkinson disease.

We also detected exaggerated beta–gamma PAC at the occipital and temporal cortices in the patients. To our knowledge, our report is the first to show exaggerated beta–gamma PAC in the occipital cortex in patients with Parkinson disease. The beta–gamma PAC in the visual cortex might have pathologic significance and might be associated with impaired visual perception[20–22] and with an accumulation of Lewy bodies in the temporal lobe[23].

Our method using MEG signals across the whole cortex successfully characterized the pathologic changes in beta–gamma PAC and beta-band power associated with the motor symptoms of Parkinson disease.

Excessive beta oscillations in the basal ganglia have been linked to Parkinson disease; however, in our patients with Parkinson disease and the matched HSPs, cortical beta oscillations during the resting state did not differ. In studies using scalp electroencephalography, no significant differences in beta-band power were observed in patients with Parkinson disease compared with HSPs[14,15,22]. Here, we estimated cortical currents from magnetic signals and used a more finely divided cortical map than had been previously used [5,25].

In previous studies that used scalp electroencephalography, electrocorticography, and MEG during the resting state in patients with Parkinson disease, cortical beta-band power was reported not to correlate with clinical motor scores[26], to vary independently of changes in motor symptoms[12], and not to differ between the on and off cycles[14,24]. In our study, beta-band power in the sensorimotor cortex did not significantly explain Parkinsonian motor symptoms, consistent with findings in those previous studies.

Although our method was successful in identifying beta–gamma PAC as characteristic of Parkinson disease, it has some limitations. First, we allowed study patients to continue taking their medications, including dopamine agonists, and thus the beta–gamma PAC in the primary motor cortex might have been suppressed in the patients. The dopamine agonists are known to suppresses exaggerated PAC in the subthalamic nucleus and the precentral gyrus in patients with Parkinson disease.[7,14,15,27] The beta–gamma PAC in Parkinson disease might therefore be underestimated in our patients. Second, the MEG signals were occasionally contaminated by noise resulting from muscle tension or head movement during recording. Procedural factors might thus have affected the number of patients judged to have severe symptoms.

Conclusions

Our results demonstrate that beta–gamma PAC measured during the resting state in the sensorimotor and visual cortices is a biomarker for Parkinson disease. As a non-invasive measure, PAC estimated from MEG signals could help to monitor a patient's symptoms and reveal the pathology behind Parkinson disease.

Methods

Participants We recruited patients with Parkinson disease from the Neurosurgery and Neurology departments of Osaka University Hospital, Osaka, Japan. HSPs were recruited through a web page hosted by the university.

Trained neurologists examined all patients with Parkinson disease and ensured that they met the Parkinson's UK Brain Bank criteria[28]. We excluded patients who had essential tremors and limb paralysis because those symptoms could change the PAC[9]. Trained clinicians used the MDS-UPDRS-III to assess motor impairments in the patients[29]. We did not require patients to stop their medications to participate. The total dose of dopaminergic antiparkinsonian drugs was converted to a levodopa equivalent daily dose.[30]

HSPs had to meet these inclusion criteria: (1) Japanese ethnicity; (2) 50 years of age or older; (3) no personal or familial diagnostic history of psychiatric disorder and no consultation with a psychiatrist, psychotherapist, neurologist, or neurosurgeon; (4) no personal or familial history of psychotropic drug use, including sleeping pills, anxiolytics, antidepressants, and antipsychotics; (5) no history of oral steroid or immunosuppressant use; (6) no history of syncope; (7) no history of organic cerebral disorders, including brain tumours or strokes; (8) no history of head injuries; (9) no history of meningitis; (10) no history of movement, sensory, or gait disturbances; (11) no history of spinal disease or arthropathy; (12) no history of thyroid disease; (13) no history of hypertension; and (14) no history of chronic liver disease or chronic kidney disease. We excluded participants if they could not remain still during the MEG recording, if they slept during the recording, or if the MEG data could not be acquired because of problems with the machine.

The study adhered to the Declaration of Helsinki and was performed in accordance with protocols approved by the Research Ethics Committee of the Osaka University Clinical Trial Centre (no. 14448, UMIN000022957). Each participant provided written informed consent after being informed of the study's purpose. For the patients who were unable to make their own decisions about participation in the study, a consent of their legal guardian was requested. Though, all patients who participated in this study had a normal cognitive and decision ability and were able to give their own consent for the participation.

MEG data acquisition MEG data were acquired using a 160-channel whole-head MEG system (MEG Vision NEO, Yokogawa Electric Corporation, Tokyo, Japan). Each participant took a supine position in a magnetically shielded room, where 5 head-marker coils were attached to their face before MEG recording started. Before and after each MEG recording, the positions of the head-marker coils were measured to determine the position and orientation of the MEG sensors relative to the head. The maximum acceptable difference in position from recording start to recording end was 5 mm. To align MEG data with individual magnetic resonance imagining data (T1 weighted; Signa HDxt Excite 3.0 T, GE Healthcare UK Ltd., Buckinghamshire, UK), we scanned the three-dimensional facial surface and 50 points on each participant's scalp (FastSCAN Cobra, Polhemus, Colchester, Vermont, USA). The recording-pass band was 0.1–500 Hz, with a sample rate of 2000 Hz.

All participants were instructed to remain awake in a resting state in the MEG scanner with eyes closed and without thinking about anything in particular. The instruction to keep eyes closed was designed to avoid artefacts from eye blinking. With participants in this state, continuous MEG data were acquired for more than 240 seconds.

Pre-processing of MEG signals We applied the continuously adjusted least-squares method,[31] performed with the MEG Laboratory software (Yokogawa Electric Corporation) using two reference magnetometers, to eliminate environmental (offline) noise. We used Brainstorm[32] with default parameters for MEG data pre-processing and MEG source imaging.

Of the original 160 channels, we excluded 10 in the temporal region for all participants because those channels were easily contaminated by muscle artefacts. MEG data resampling at 1000 Hz and high-pass filtering at 0.5 Hz were performed for baseline correction. In an independent component analysis, we used the Infomax algorithm implemented in Brainstorm to isolate ocular and cardiac artefacts. That algorithm calls the function runica.m from the EEGLAB toolbox[33]. Afterward, we visually inspected the MEG data to detect segments that remained contaminated by muscle artefacts or environmental noise. Contaminated segments were discarded from subsequent analyses. To eliminate powerline contamination, we applied a band-stop filter at 60 Hz with a width of 1.5 Hz to the clean MEG data. Finally, to increase calculation speed, the MEG data were resampled at 500 Hz. Data with irremediable artefacts, usually caused by dental implants, were excluded from further analysis.

Estimation of cortical currents from MEG signals Scalp and cortical surfaces were extracted from magnetic resonance imagining volume data. For each envelope, we used the FreeSurfer software (Martinos Center, Charlestown, Massachusetts, USA)[34] with default parameter settings to obtain a surface triangulation that was subsequently imported into Brainstorm. The individual high-resolution cortical surfaces (approximately 75,000 vertices per surface) were downsampled to approximately 15,000 triangular

vertices (also using a Brainstorm process) to serve as image supports for MEG source imaging. We then used Brainstorm's multilinear registration procedure to transform each vertex location into the FreeSurfer average anatomy[35] (15,002 vertices). Forward modelling of the neural magnetic fields used the overlapping-sphere technique implemented in Brainstorm.[36] For MEG source imaging, we applied the minimum-norm estimation method to the pre-processed data and estimated the cortical current for each vertex. Further analyses were based on the estimated cortical current.

Evaluation of power The power of the estimated current at each cortical point was calculated for 3 frequency bands (alpha, 8–12 Hz; beta, 13–30 Hz; gamma, 50–100 Hz). For resting-state data, we divided each estimated cortical current into overlapping 1-second time windows shifted by 200 milliseconds. We applied a Hamming window and fast Fourier transform to each time window to obtain a power spectrum. A Z score normalization was performed on the whole brain for each frequency band.

The power values at each cortical point were grouped into 360 cortical areas from the Human Connectome Project (HCP) map of cortices[37] and were averaged for each cortical area.

Evaluation of PAC We used the SI[19] to evaluate the intensity of the PAC. The SI is defined as

$$\mathrm{SI} = \left| \frac{1}{N} \sum_{t=1}^{N} e^{i(\theta phs(t) - \theta amp(t))} \right|,$$

where N is the number of time points in each time window for analysis, $\theta_{phs}(t)$ is the phase value of the lower-frequency-band time series at time point *t,* and $\theta_{amp}(t)$ is the phase value of the fluctuations in the gamma amplitude time series at time *t.*

We evaluated the phase values of the alpha and beta bands. Using a Hilbert transform, we filtered the gamma amplitude by the alpha or beta frequency band to obtain phase values. To calculate the SI values, we subtracted the $\theta_{phs}(t)$ and $\theta_{amp}(t)$ of the alpha or beta frequency band—that is, the SI values correspond to the PAC between the gamma amplitude and the alpha or beta phase. The SI values varied between 0 and 1, with 0 indicating completely desynchronized phases and 1 indicating perfectly synchronized phases.

We used a 236-second time window to evaluate the SI value. The averaged SI values for each cortical vertex were grouped into 360 cortical areas as already described for the evaluation of power.

Prediction of MDS-UPDRS-III score from PAC and power We estimated how predictive both beta–gamma PAC and beta-band power during a resting state were with respect to the severity of motor impairments in patients with Parkinson disease. We used MDS-UPDRS-III scores for akinesia to quantify motor impairments, derived as the sum of 3.4, finger tapping; 3.5, hand movements; 3.6, pronation–supination movements of hands; 3.7, toe tapping; and 3.8, leg agility. We used the area-averaged SI values in the sensorimotor areas in which significant SI values were present to assess PAC. In the same regions, we used averaged Z scores to assess beta-band power. A Pearson correlation coefficient was used to quantify the relationship between MDS-UPDRS-III scores for akinesia and the SI values or Z scores.

Statistical analysis Statistical analyses were performed in the MATLAB R2015b software (MathWorks, Natick, Massachusetts, USA). To evaluate the significance of PAC, we also estimated the SI values expected by chance by using phase-shuffled data to estimate phase-shuffled SI.[38,39] The 100 phase-shuffled SI values that we calculated were compared with the original SI values using 2-tailed paired *t*-tests. To control for false discovery rates[40] across cortical areas, we calculated corrected *P* values at each cortical area by comparing the distribution of *t* values with the distribution of permutated *t* values expected by chance.

A 2-way analysis of variance was performed on the Z score power of each cortical area for the selected frequency bands and the participant groups. To control for false discovery rates across cortical areas, we calculated corrected *P* values at each cortical area, comparing the distribution of *F* values with the distribution of permutated *F* values expected by chance. All analyses were 2-sided, with a significance level of 0.05.

We used permutation testing to determine the significance of correlations between MDS-UPDRS-III scores for akinesia and the PAC or power, evaluating whether more or fewer significant correlations were observed than would be expected by chance. The SI values and Z scores were randomly permuted for participants while the MDS-UPDRS-III scores were kept the same. We computed a surrogate correlation coefficient based on those shuffled data and repeated the procedure for 2000 permutations, yielding a null distribution of numbers of significant correlations. Significant correlation coefficients were then defined as those that differed significantly from the null distribution.

The number of patients included in the study was calculated in an a priori power analysis in the G*Power program[41]. Our null hypothesis—that the correlation coefficients

would differ from 0 in the negative direction—was based on previous studies.[12,27] The effect size (ρ), power to be achieved (β), and probability of an alpha error were set to 0.60, 0.80, and 0.05 respectively. We determined the sample size to be 30, with an expected loss of 30%.

References

1 Williams, D. *et al.* Dopamine-dependent changes in the functional connectivity between basal ganglia and cerebral cortex in humans. *Brain* **125** (2002). URL 10.1093/brain/awf156.

2 Blumenfeld, Z. & Bronte-Stewart, H. High Frequency deep brain stimulation and neural rhythms in Parkinson's disease. *Neuropsychol Rev* **25** (2015). URL 10.1007/s11065–015–9308–7.

3 Little, S. & Brown, P. What brain signals are suitable for feedback control of deep brain stimulation in Parkinson's disease? *Ann N Y Acad Sci* **1265** (2012). URL 10.1111/j.1749–6632.2012.06650.x.

4 Pavlides, A., Hogan, S.J. & Bogacz, R. Computational models describing possible mechanisms for generation of excessive beta oscillations in Parkinson's disease. *PLoS Comput Biol* **11** (2015). URL 10.1371/journal.pcbi.1004609.

5 Stoffers, D. *et al.* Slowing of oscillatory brain activity is a stable characteristic of Parkinson's disease without dementia. *Brain* **130** (2007). URL 10.1093/brain/awm034.

6 Yang, A.I., Vanegas, N., Lungu, C. & Zaghloul, K.A. Beta-coupled high-frequency activity and beta-locked neuronal spiking in the subthalamic nucleus of Parkinson's disease. *J Neurosci* **34** (2014). URL 10.1523/JNEUROSCI.1895–14.2014.

7 Lopez-Azcarate, J. *et al.* Coupling between beta and high-frequency activity in the human subthalamic nucleus may be a pathophysiological mechanism in Parkinson's disease. *J Neurosci* **30** (2010). URL 10.1523/JNEUROSCI.5459–09.2010.

8 de Hemptinne, C. *et al.* Exaggerated phase-amplitude coupling in the primary motor cortex in Parkinson disease. *Proc Natl Acad Sci U S A* **110** (2013). URL 10.1073/pnas.1214546110.

9 Kondylis, E.D. *et al.* Movement-related dynamics of cortical oscillations in Parkinson's disease and essential tremor. *Brain* **139** (2016). URL 10.1093/brain/aww144.

10 Canolty, R.T. & Knight, R.T. The functional role of cross-frequency coupling. *Trends Cogn Sci* **14** (2010). URL 10.1016/j.tics.2010.09.001.

11 Yanagisawa, T. *et al.* Regulation of motor representation by phase-amplitude coupling in the sensorimotor cortex. *J Neurosci* **32,** 15467–15475, doi:10.1523/JNEUROSCI.2929–12.2012 (2012).

12 de Hemptinne, C. *et al.* Therapeutic deep brain stimulation reduces cortical phase-amplitude coupling in Parkinson's disease. *Nat Neurosci* **18,** 779–786, doi:10.1038/nn.3997 (2015).

13 Bouthour, W. *et al.* Biomarkers for closed-loop deep brain stimulation in Parkinson disease and beyond. *Nature reviews. Neurology* **15,** 343–352, doi:10.1038/s41582–019–0166–4 (2019).

14 Swann, N. C. *et al.* Elevated synchrony in Parkinson disease detected with electroencephalography. *Ann Neurol* **78,** 742–750, doi:10.1002/ana.24507 (2015).

15 Miller, A. M. *et al.* Effect of levodopa on electroencephalographic biomarkers of the parkinsonian state. *J Neurophysiol* **122,** 290–299, doi:10.1152/jn.00141.2019 (2019).

16 Roux, F., Wibral, M., Singer, W., Aru, J. & Uhlhaas, P. J. The Phase of Thalamic Alpha Activity Modulates Cortical Gamma-Band Activity: Evidence from Resting-State MEG Recordings. *J Neurosci* **33,** 17827–17835, doi:10.1523/JNEUROSCI.5778–12.2013 (2013).

17 van Wijk, B. C., Jha, A., Penny, W. & Litvak, V. Parametric estimation of cross-frequency coupling. *J Neurosci Methods* **243,** 94–102, doi:10.1016/j.jneumeth.2015.01.032 (2015).

18 Daume, J., Gruber, T., Engel, A. K. & Friese, U. Phase-Amplitude Coupling and Long-Range Phase Synchronization Reveal Frontotemporal Interactions during Visual Working Memory. *J Neurosci* **37,** 313–322, doi:10.1523/JNEUROSCI.2130–16.2016 (2017).

19 Cohen, M. X. Assessing transient cross-frequency coupling in EEG data. *J Neurosci Methods* **168,** 494–499, doi:S0165–0270(07)00523–7 [pii]10.1016/j.jneumeth.2007.10.012 (2008).

20 Goldman, J. G. *et al.* Visuoperceptive region atrophy independent of cognitive status in patients with Parkinson's disease with hallucinations. *Brain* **137,** 849–859, doi:10.1093/brain/awt360 (2014).

21 Gasca-Salas, C., Clavero, P., Garcia-Garcia, D., Obeso, J. A. & Rodriguez-Oroz, M. C. Significance of visual hallucinations and cerebral hypometabolism in the risk of dementia in Parkinson's disease patients with mild cognitive impairment. *Human brain mapping* **37,** 968–977, doi:10.1002/hbm.23080 (2016).

22 Firbank, M. J. *et al.* Reduced occipital GABA in Parkinson disease with visual hallucinations. *Neurology* **91,** e675-e685, doi:10.1212/WNL.0000000000006007 (2018).

23 Harding, A. J., Broe, G. A. & Halliday, G. M. Visual hallucinations in Lewy body disease relate to Lewy bodies in the temporal lobe. *Brain* **125,** 391–403, doi:10.1093/brain/awf033 (2002).

24 George, J. S. *et al.* Dopaminergic therapy in Parkinson's disease decreases cortical beta band coherence in the resting state and increases cortical beta band power during executive control. *Neuroimage Clin* **3,** 261–270, doi:10.1016/j.nicl.2013.07.013 (2013).

25 Bosboom, J. L. *et al.* Resting state oscillatory brain dynamics in Parkinson's disease: an MEG study. *Clin Neurophysiol* **117,** 2521–2531, doi:10.1016/j.clinph.2006.06.720 (2006).

26 Vardy, A. N. *et al.* Slowing of M1 activity in Parkinson's disease during rest and movement--an MEG study. *Clin Neurophysiol* **122,** 789–795, doi:10.1016/j.clinph.2010.10.034 (2011).

27 van Wijk, B. C. *et al.* Subthalamic nucleus phase-amplitude coupling correlates with motor impairment in Parkinson's disease. *Clin Neurophysiol* **127,** 2010–2019, doi:10.1016/j.clinph.2016.01.015 (2016).

28 Hughes, A. J., Daniel, S. E., Kilford, L. & Lees, A. J. Accuracy of clinical diagnosis of idiopathic Parkinson's disease: a clinico-pathological study of 100 cases. *J Neurol Neurosurg Psychiatry* **55,** 181–184, doi:10.1136/jnnp.55.3.181 (1992).

29 Goetz, C. G. *et al.* Movement Disorder Society-sponsored revision of the Unified Parkinson's Disease Rating Scale (MDS-UPDRS): scale presentation and clinimetric testing results. *Mov Disord* **23,** 2129–2170, doi:10.1002/mds.22340 (2008).

30 Tomlinson, C. L. *et al.* Systematic review of levodopa dose equivalency reporting in Parkinson's disease. *Mov Disord* **25,** 2649–2653, doi:10.1002/mds.23429 (2010).

31 Adachi, Y., Shimogawara, M., Higuchi, M., Haruta, Y. & Ochiai, M. Reduction of non-periodic environmental magnetic noise in MEG measurement by continuously adjusted least squares method. *IEEE Trans Appl Supercond* **11,** 669–672, doi:10.1109/77.919433 (2001).

32 Tadel, F., Baillet, S., Mosher, J. C., Pantazis, D. & Leahy, R. M. Brainstorm: a user-friendly application for MEG/EEG analysis. *Computational intelligence and neuroscience* **2011,** 879716, doi:10.1155/2011/879716 (2011).

33 Delorme, A. & Makeig, S. EEGLAB: an open source toolbox for analysis of single-trial EEG dynamics including independent component analysis. *J Neurosci Methods* **134,** 9–21, doi:10.1016/j.jneumeth.2003.10.009S0165027003003479 [pii] (2004).

34 Dale, A. M., Fischl, B. & Sereno, M. I. Cortical surface-based analysis. I. Segmentation and surface reconstruction. *NeuroImage* **9,** 179–194, doi:10.1006/nimg.1998.0395 (1999).

35 Fischl, B., Sereno, M. I., Tootell, R. B. & Dale, A. M. High-resolution intersubject averaging and a coordinate system for the cortical surface. *Human brain mapping* **8,** 272–284 (1999).

36 Huang, M. X., Mosher, J. C. & Leahy, R. M. A sensor-weighted overlapping-sphere head model and exhaustive head model comparison for MEG. *Phys Med Biol* **44,** 423–440, doi:10.1088/0031–9155/44/2/010 (1999).

37 Glasser, M. F. *et al.* A multi-modal parcellation of human cerebral cortex. *Nature* **536,** 171–178, doi:10.1038/nature18933 (2016).

38 Axmacher, N. *et al.* Cross-frequency coupling supports multi-item working memory in the human hippocampus. *Proc Natl Acad Sci U S A* **107,** 3228–3233, doi:10.1073/pnas.0911531107 (2010).

39 Edakawa, K. *et al.* Detection of Epileptic Seizures Using Phase-Amplitude Coupling in Intracranial Electroencephalography. *Sci Rep* **6,** 25422, doi:10.1038/srep25422 (2016).

40 Benjamini, Y. & Hochberg, Y. Controlling the false discovery rate - a practical and powerful approach to multiple testing. *J R Stat Soc B-Stat Methodol* **57,** 289–300 (1995).

41 Faul, F., Erdfelder, E., Buchner, A. & Lang, A. G. Statistical power analyses using G*Power 3.1: tests for correlation and regression analyses. *Behav Res Methods* **41,** 1149–1160, doi:10.3758/BRM.41.4.1149 (2009).

Acknowledgments

This research was conducted under a grant from the Japan Agency for Medical Research and Development (AMED) (19dm0207070h0001). It was also supported in part by the following organizations and programs: Japan Science and Technology Agency's Precursory Research for Embryonic Science and Technology (JPMJPR1506), Core Research for Evolutional Science and Technology (JPMJCR18A5), and Exploratory Research for Advanced Technology (JPMJER1801); Grants-in-Aid for Scientific Research from the Japan Society for the Promotion of Science (JP24700419, JP26560467, JP22700435, JP15H05710, JP18H04085, and JP18H05522); AMED (19dm0307103 and 19de0107001); and the Magnetic Health Science Foundation (29210).

Author contributions

TY designed and conceptualized the study. MT, NT, SO, MM, NH, YK, and RH collected data. RF wrote the code for the analysis. MT analysed data, did the statistical analysis, and prepared all figures and tables. TY interpreted data. MT and TY performed the literature search and wrote the manuscript. MI, HM, and HK reviewed the manuscript.

Declarations of interest

The authors have no competing interests to declare.

Data availability

The data that support the findings of this study are openly available at http://doi.org/10.6084/m9.figshare.12986111.

Corresponding author:

Takufumi Yanagisawa, MD, PhD

Department of Neurosurgery

Osaka University Graduate School of Medicine

2–2 Yamadaoka, Suita

Osaka 565-0871 Japan

Email: tyanagisawa@nsurg.med.osaka-u.ac.jp

Supplementary Files

This is a list of supplementary files associated with this preprint. Click to download.

- supplementarytable.docx